Comparative Studies on Exchange Reactions of Hexafluoroacetylacetonate in Bis(hexafluoroacetylacetonato)(dimethyl sulfoxide)dioxouranium(VI) in Nonaqueous Solvent and Supercritical CO$_2$

Yoshihiro Kachi,[†] Yoshihito Kayaki,[‡] Takehiko Tsukahara,[§] Takao Ikariya,[‡] and Yasuhisa Ikeda*[,†]

Research Laboratory for Nuclear Reactors, Tokyo Institute of Technology, 2-12-1-N1-34 O-okayama, Meguro-ku, Tokyo 152-8550, Japan, Department of Applied Chemistry, Tokyo Institute of Technology, 2-12-1-S1-39 O-okayama, Meguro-ku, Tokyo 152-8552, Japan, Department of Applied Chemistry, The University of Tokyo, 7-3-1, Hongo, Bunkyo-ku, Tokyo, 113-8656, Japan

Exchange reactions of hexafluoroacetylacetonate (hfacac) in UO$_2$(hfacac)$_2$DMSO (DMSO = dimethyl sulfoxide) in *o*-C$_6$D$_4$Cl$_2$ and supercritical CO$_2$ (sc-CO$_2$) have been studied using the NMR line-broadening method to compare reactivity in a nonaqueous solvent with that in sc-CO$_2$. It was found that the exchange rates of hfacac in both systems are dependent on the concentration of the enol isomer ([Henol]) of hexafluoroacetylacetone and become slow with an increase in the concentration of free DMSO ([DMSO]). The exchange reaction between free and coordinated DMSO in UO$_2$(hfacac)$_2$DMSO has been also examined in *o*-C$_6$D$_4$Cl$_2$ and sc-CO$_2$. As a result, the exchange rate of DMSO was found to depend on [DMSO]. From these results, the hfacac exchange reactions in UO$_2$(hfacac)$_2$DMSO in *o*-C$_6$D$_4$Cl$_2$ and sc-CO$_2$ were proposed to proceed through the mechanism that the ring-opening for one of two coordinated hfacac in UO$_2$(hfacac)$_2$DMSO is the rate-determining step, and the resulting vacant site is coordinated by the incoming Henol, followed by the proton transfer from Henol to hfacac and the ring closure of unidentate hfacac. The rate constants at 60 °C and the activation parameters ($\Delta H^{\ddagger}$ and $\Delta S^{\ddagger}$) for the ring-opening path are 35.8 ± 3.2 s^{-1}, 57.8 ± 2.7 kJ·mol^{-1}, and −42.9 ± 7.7 J·mol^{-1}·K^{-1} for the *o*-C$_6$D$_4$Cl$_2$ system, and 518 ± 50 s^{-1}, 18.9 ± 1.8 kJ·mol^{-1}, and −138 ± 5 J·mol^{-1}·K^{-1} for the sc-CO$_2$ system, respectively. Differences in kinetic parameters between sc-CO$_2$ and *o*-C$_6$D$_4$Cl$_2$ systems were proposed to be attributed to the solute–solvent interactions such as Lewis acid–Lewis base interactions and hydrogen bondings between sc-CO$_2$ and β-diketones.

Introduction

Supercritical CO$_2$ (sc-CO$_2$) has been extensively studied as a medium for organic reactions, extractions, dyeing, washing, and drying.[1−4] Especially, in the extraction field, sc-CO$_2$ has become of interest as an alternative to organic solvents, for example, as a separation medium for metal ions in spent nuclear fuel reprocessing or radioactive waste treatment.[5−11] However, it is well-known that the direct extraction of metal ions to the sc-CO$_2$ phase is difficult.[9−11]

(1) Kiran, E.; Sengeers, J. M. H. L. *Supercritical Fluids-Fundamentals for Application*; Kluwer: Dordrecht, The Netherlands, 1994.
(2) Hutchenson, K. W.; Foster, N. R. *Innovations in Supercritical Fluids*; American Chemical Society: Washington, 1995.
(3) Jessop, P. G.; Ikariya, T.; Noyori, R. *Chem. Rev.* **1999**, *99*, 475−494.
(4) Kajimoto, O. *Chem. Rev.* **1999**, *99*, 355−389.

(5) Carrott, M. J.; Waller, B. E.; Smart, N. G.; Wai, C. M. *Chem. Commun.* **1998**, 373−374.
(6) Meguro, Y.; Iso, S.; Sasaki, T.; Yoshida, Z. *Anal. Chem.* **1998**, *70*, 774−779.
(7) Tomioka, O.; Meguro, Y.; Enokida, Y.; Yamamoto, I. Yoshida, Z. *J. Nucl. Sci. Technol.* **2001**, *38*, 1097−1102.
(8) Galand, N.; Wipff, G. *J. Phys. Chem. B* **2005**, *109*, 277−287.
(9) Lin, Y.; Brauer, R. D.; Laintz, K. E.; Wai, C. M. *Anal. Chem.* **1993**, *65*, 2549−2551.
(10) Lin, Y.; Wai, C. M. *Anal. Chem.* **1994**, *66*, 1971−1975.
(11) Darr, J. A.; Poliakoff, M. *Chem. Rev.* **1999**, *99*, 495−541.

Hence, the techniques using sc-CO_2 containing extractants such as tributyl phosphate and β-diketones have been developed extensively.[5−8]

To use extensively sc-CO_2 as a medium for the extraction methods, it is necessary to clarify the factors for controlling the solubility of solutes such as extractants and their metal complexes in sc-CO_2 and to design the CO_2-philic compounds with selectivity toward metal ions. Thus, many studies on solute−solvent interactions in sc-CO_2 have been performed.[12−30] Such studies have revealed that the solubility of compounds in sc-CO_2 is enhanced by fluorination.[10,21−25] Moreover, it has been elucidated that hydrocarbons with carbonyl group(s) such as aldehydes, ketones, and acetates have the Lewis acid−Lewis base (LA−LB) interactions and hydrogen bondings with sc-CO_2 and that the LA−LB interactions of solutes play important roles for the enhancement of solubility of solutes.[26−30] Recently, we reported that the CO_2-philicity of solutes in sc-CO_2 can be estimated from chemical shifts of ^{13}C NMR of CO_2 in sc-CO_2 containing solutes.[31] More recently, we measured the Raman spectra of sc-CO_2 containing β-diketones and their uranyl complexes, and clarified that the LA−LB interactions between carbonyl oxygens of β-diketones and CO_2 carbon, and the hydrogen bonding between −OH of β-diketones and CO_2 oxygen are formed.[32] Furthermore, on the basis of this knowledge, we measured the Raman spectra of sc-CO_2 containing compounds with different donicity (donor number, DN) such as acetic anhydride, methyl acetate, N,N-dimethylformamide (DMF), dimethyl sulfoxide (DMSO), and found out that the

extent of red shifts in Raman bands of CO_2 is used as the measure for the strength of LA−LB interactions formed between CO_2 and the solutes in sc-CO_2.[32]

In spite of many studies on the solute−solvent interactions as described above, complex formation reactions of metal ions with extractants and ligand exchange reactions of metal complexes in sc-CO_2, which are the most fundamental data for understanding extraction mechanisms of metal ions in sc-CO_2 medium, have not been studied sufficiently.[33−35]

For uranyl complexes, many studies on ligand exchange reactions have been undertaken in aqueous and nonaqueous solvents.[36−58] Especially, inter- and/or intramolecular exchange reactions of β-diketonates in $UO_2(\beta\text{-diketonato})_2L$ [β-diketonates = acetylacetonate (acac), dibenzoylmethanate (dbm), hexafluoroacetylacetonate (hfacac), L = oxygen donor ligands such as DMSO, DMF, and so on] have been studied in nonaqueous solvents.[42,47−50,52] In the exchange reactions of acac in $UO_2(acac)_2L$ (L = DMSO, DMF) in $o\text{-}C_6D_4Cl_2$, we found that the apparent first-order exchange rate constants (k_{ex}) increase and approach limiting values with an increase in concentration of the enol isomer of acetylacetone (Hacac) and that the k_{ex} values decrease with increasing concentrations of free L.[50,52] From such results, we proposed the exchange reaction mechanism that the ring-opening for one of two coordinated acac in $UO_2(acac)_2L$ is the rate-

(12) Blitz, J. P.; Yonker, C. R.; Smith, R. D. *J. Phys. Chem.* **1989**, *93*, 6661−6665.
(13) Fulton, J. L.; Yee, G. G.; Smith, R. D. *J. Am. Chem. Soc.* **1991**, *113*, 8327−8334.
(14) Sun, Y.; Bennet, G.; Johnston, K. P.; Fox, M. A. *J. Phys. Chem.* **1992**, *96*, 10001−10007.
(15) Meredith, J. C.; Johnston, K. P.; Seminario, J. M.; Kazarian, S. G.; Eckert, C. A. *J. Phys. Chem.* **1996**, *100*, 10837−10848.
(16) Diep, P.; Jordan, K. D.; Johnson, J. K.; Beckman, E. J. *J. Phys. Chem. A* **1998**, *102*, 2231−2236.
(17) Nelson, M. R.; Borkman, R. F. *J. Phys. Chem. A* **1998**, *102*, 7860−7863.
(18) Danten, Y.; Tassaing, T.; Besnard, M. *J. Phys. Chem. A* **2002**, *106*, 11831−11840.
(19) Raveendran, P.; Wallen, S. L. *J. Phys. Chem. B* **2003**, *107*, 1473−1477.
(20) Raveendran, P.; Ikushima, Y.; Wallen, S. L. *Acc. Chem. Res.* **2005**, *38*, 478−485.
(21) Yee, G. G.; Fulton, J. L.; Smith, R. D. *J. Phys. Chem.* **1992**, *96*, 6172−6181.
(22) Smart, N. G.; Carleson, T.; Kast, T.; Clifford, A. A.; Burford, M. D.; Wai, C. M. *Talanta* **1997**, *44*, 137−150.
(23) Wai, C. M.; Wang, S. *J. Chromatogr. A* **1997**, *785*, 369−383.
(24) Dardin, A.; DeSimone, J. M.; Samulski, E. T. *J. Phys. Chem. B* **1998**, *102*, 1775−1780.
(25) Yonker, C. R.; Palmer, B. J. *J. Phys. Chem. A* **2001**, *105*, 308−314.
(26) Akimoto, S.; Kajimoto, O. *Chem. Phys. Lett.* **1993**, *209*, 263−268.
(27) Felker, P. M.; Maxton, P. M.; Schaeffer, M. W. *Chem. Rev.* **1994**, *94*, 1787−1805.
(28) Lalanne, P.; Rey, S.; Cansell, F.; Tassaing, T.; Besnard, M. *J. Supercrit. Fluids* **2001**, *19*, 199−207.
(29) Raveendran, P.; Wallen, S. L. *J. Am. Chem. Soc.* **2002**, *124*, 12590−12599.
(30) Blatchford, M. A.; Raveendran, P.; Wallen, S. L. *J. Phys. Chem. A* **2003**, *107*, 10311−10323.
(31) Tsukahara, T.; Kayaki, Y.; Ikariya, T.; Ikeda, Y. *Angew. Chem., Int. Ed.* **2004**, *43*, 3719−3722.
(32) Kachi, Y.; Tsukahara, T.; Kayaki, Y.; Ikariya, T.; Ikeda, Y. *J. Supercrit. Fluids* **2007**, *40*, 20−26.

(33) Inada, Y.; Sato, H.; Liu, S.; Horita, T.; Funahashi, S. *J. Phys. Chem. A* **2003**, *107*, 1525−1531.
(34) Inada, Y.; Horita, T.; Yokooka, Y.; Funahashi, S. *J. Supercrit. Fluids* **2004**, *31*, 175−183.
(35) Liu, S.; Inada, Y.; Funahashi, S. *J. Supercrit. Fluids* **2004**, *30*, 237−246.
(36) Gordon, G.; Taube, H. *J. Inorg. Nucl. Chem.* **1961**, *16*, 272−278.
(37) Bowen, R. P.; Lincoln, S. F.; Williams, E. H. *Inorg. Chem.* **1976**, *15*, 2126−2129.
(38) Lincoln, S. F. *Pure Appl. Chem.* **1979**, *51*, 2059−2065.
(39) Honan, G. J.; Lincoln, S. F.; Williams, E. H. *Aust. J. Chem.* **1979**, *32*, 1851−1855.
(40) Ikeda, Y.; Soya, S.; Fukutomi, H. *J. Inorg. Nucl. Chem.* **1979**, *41*, 1333−1337.
(41) Kramer, G. M.; Dines, M. B.; Melchior, M. T.; Maas, Jr. E. T. *Inorg. Chem.* **1981**, *20*, 3−6.
(42) Kramer, G. M.; Maas, E. T., Jr.; Dines, M. B. *Inorg. Chem.* **1981**, *20*, 1418−1420.
(43) Kramer, G. M.; Dines, M. B.; Kaldor, A.; Hall, R.; McClure. D. *Inorg. Chem.* **1981**, *20*, 1421−1426.
(44) Kramer, G. M.; Maas, E. T., Jr. *Inorg. Chem.* **1981**, *20*, 3514−3516.
(45) Bray, R. G.; Kramer, G. M. *Inorg. Chem.* **1983**, *22*, 1843−1848.
(46) Doine, H.; Ikeda, Y.; Tomiyasu, H.; Fukutomi, H. *Bull. Chem. Soc. Jpn.* **1983**, *56*, 1989−1994.
(47) Ikeda, Y.; Tomiyasu, H.; Fukutomi, H. *Bull. Chem. Soc. Jpn.* **1983**, *56*, 1060−1066.
(48) Ikeda, Y.; Tomiyasu, H.; Fukutomi, H. *Bull. Chem. Soc. Jpn.* **1984**, *57*, 2925−2929.
(49) Ikeda, Y.; Tomiyasu, H.; Fukutomi, H. *Inorg. Chem.* **1984**, *23*, 1356−1360.
(50) Ikeda, Y.; Tomiyasu, H.; Fukutomi, H. *Inorg. Chem.* **1984**, *23*, 3197−3202.
(51) Lincoln, S. F. White, A. *Inorg. Chim. Acta* **1985**, *110*, 107−112.
(52) Fukutomi, H.; Ikeda, Y. *Inorg. Chim. Acta* **1986**, *115*, 223−227.
(53) White, A.; Lincoln, S. F. *J. Chem. Soc., Dalton Trans.* **1987**, 2885−2888.
(54) Farkas, I.; Grenthe, I. *J. Phys. Chem. A* **2000**, *104*, 1201−1206.
(55) Vallet, V.; Wahlgren, U.; Schimmelpfennig, B.; Szabó, Z.; Grenthe, I. *J. Am. Chem. Soc.* **2001**, *123*, 11999−12008.
(56) Vallet, V.; Wahlgren, U.; Szabó, Z.; Grenthe, I. *Inorg. Chem.* **2002**, *41*, 5626−5633.
(57) Vallet, V.; Szabó, Z.; Grenthe, I. *J. Chem. Soc., Dalton Trans.* **2004**, 3799−3907.
(58) Szabó, Z.; Toraishi, T.; Vallet, V.; Grenthe, I. *Coord. Chem. Rev.* **2006**, *250*, 784−815.

determining step, and the resulting vacant site is coordinated by the entering Hacac, followed by the proton transfer from Hacac to acac and the ring closure of unidentate acac.[50,52]

As mentioned above, there are solute−solvent interactions between CO_2 and β-diketones or oxygen donor compounds.[31,32] Hence, such interactions should affect ligand exchange reactions in $UO_2(\beta$-diketonato$)_2$L complexes in sc-CO_2 and lead to different phenomena from those in the nonaqueous solvents. However, little information is available concerning comparative studies on the exchange reactions of uranyl complexes in nonaqueous solvents and sc-CO_2.[33] Such data should be helpful for understanding the differences in the reactivity of solutes in nonaqueous solvents and sc-CO_2 and for designing supercritical extraction processes of metal ions.

In the present study, hence, we have examined the ligand exchange reactions in $UO_2(hfacac)_2DMSO$ in o-$C_6D_4Cl_2$ and sc-CO_2 to compare the reactivity of the $UO_2(hfacac)_2DMSO$ in both media.

Experimental Section

Materials. The $UO_2(hfacac)_2DMSO$ complex was synthesized by the same method as reported previously.[59] Hexafluoroacetylacetone (Hhfacac, Wako Pure Chemical Ind. Ltd., 99%) was purified by distillation. Dimethyl sulfoxide (Wako, 99%), DMSO-d_6 (Kanto Chemical Co., Inc., 98 atom% D), o-$C_6H_4Cl_2$ (Kanto Chemical Co., Inc., 99%), o-$C_6D_4Cl_2$ (Sigma-Aldrich Co., 98 atom% D), and CD_2-Cl_2 (Kanto, 99.8 atom% D) were stored over 4 Å molecular sieves prior to use. Pure grade CO_2 (Tomoe Shokai Co., Ltd., 99.999%) was used.

Measurements of NMR and Raman Spectra of o-$C_6D_4Cl_2$ and sc-CO_2 Containing Solutes. ^1H and ^{19}F NMR spectra of o-C_6D_4-Cl_2 containing solutes were measured using a JEOL JNM LA 300 WB FT-NMR spectrometer at atmospheric pressure in the temperature range from 40 to 120 °C. In the sc-CO_2 system, the pressure was controlled at 25 MPa in the same temperature range. A zirconia cell (ZC inner diameter, 5.4 mm; outer diameter, 9.0 mm; length, 152.0 mm) was used as a high-pressure NMR sample tube. NMR measurements were performed by the following procedures: (i) putting $UO_2(hfacac)_2DMSO$ into the ZC, (ii) inserting a glass capillary (diameter, 4.2 mm; length, 142.9 mm) containing DMSO-d_6 as an internal lock into the ZC, (iii) adding Hhfacac to the ZC by using a microsyringe, (iv) fixing the ZC to the Ti−Al sample holder and connecting the sample holder with a stainless steel inlet tube, (v) charging CO_2 gas into the ZC using a syringe pump (ISCO Model-260D). The pressure and temperature of the samples were controlled by using a back-pressure regulator (JASCO 880−81) and by providing heated air from the lower part of probe, respectively.[31,60]

Raman spectra of $UO_2(hfacac)_2DMSO$ in o-$C_6H_4Cl_2$ were measured by a Raman spectrophotometer (JASCO RMP-200) equipped with a single monochromatic spectrograph system with a grating of 1800 lines/mm at atmospheric pressure. In the case of the sc-CO_2 system, we used a high-pressure cell (TAIATSU Glass Co., Ltd.), and the pressure and temperature were controlled at 25 MPa and 40 °C. The high-pressure cell body (volume = 819 cm³) is made from stainless steel (SUS316) with three sapphire windows.

The optical path length of the cell and the volume of the sample are 2.6 cm and 8.1 cm³, respectively. The light source is a semiconductor laser (Nd:YVO₄), operating at 532 nm with a power of 100 mW. The high-pressure Raman measurements were performed by the same method as reported previously.[32]

Measurements of the Keto−Enol Equilibrium Constant for Hexafluoroacetylacetone. Hexafluoroacetylacetone has keto and enol forms (abbreviated as Keto and Henol). The tautomeric ratios of Hhfacac (2.83×10^{-2} M, M = mol·dm⁻³) in o-$C_6D_4Cl_2$ were measured from the areas of ^{19}F NMR peaks due to the −CF₃ of Keto and Henol in the range from 40 to 120 °C. The same measurements in sc-CO_2 containing Hhfacac (2.96×10^{-2} M) were carried out in the range from 40 to 120 °C at 25 MPa. The equilibrium constants, $K_{keto-enol}$ = [Keto]/[Henol], were evaluated from the ratios measured.

Plots of ln $K_{keto-enol}$ versus the reciprocal temperature are shown in Figure S1 in the Supporting Information. The values of ΔH and ΔS for $K_{keto-enol}$ were obtained as 21.9 ± 1.3 kJ·mol⁻¹ and 28.4 ± 3.7 J·K⁻¹·mol⁻¹ in o-$C_6D_4Cl_2$, and 14.5 ± 1.1 kJ·mol⁻¹ and 7.3 ± 3.1 J·K⁻¹·mol⁻¹ in sc-CO_2.

Kinetic Analyses. Kinetic analyses of ligand exchange reactions in $UO_2(hfacac)_2DMSO$ were carried out using a computer program based on a two-site exchange as mentioned previously.[52,61] In the present study, *gNMR* was used as a computer program.[62] Input parameters for this program are the chemical shifts and the full widths at half-maximum (fwhm) of signals corresponding to the coordinated and free ligands. In o-$C_6D_4Cl_2$, the chemical shifts and fwhm at a temperature, in which the exchange is negligibly slow reactions, are used as the input parameters. In the sc-CO_2 system, the chemical shifts and fwhm of NMR signals in sc-CO_2 containing only free ligand (Hhfacac and DMSO) and $UO_2(hfacac)_2DMSO$ were measured at each temperature and used as input data, because NMR resolution becomes lower due to the convection of sc-CO_2 with the approach to the critical density of CO_2 with an increase in temperature.[63] The apparent first-order rate constants (k_{ex}) for the ligand exchange reactions were obtained from the best-fit τ-values by using the following equations:

$$\tau = \tau_c P_f = \tau_f P_c, \quad k_{ex} = 1/\tau_c \qquad (1)$$

where τ and P with the subscripts of c and f express the mean lifetimes and the mole fractions of the coordinated ligand and the free one, respectively.

Results and Discussion

Structure of $UO_2(hfacac)_2DMSO$ in o-$C_6D_4Cl_2$ and sc-CO_2 Containing Free Hhfacac. It has been known that the $UO_2(hfacac)_2L$ (L = unidentate ligands) complexes have a pentagonal bipyramidal structure and cause the following displacement reactions in nonaqueous solvents,

$$UO_2(hfacac)_2L + L' = UO_2(hfacac)_2L' + L \qquad (2)$$

where L′ is L itself or other unidentate ligands.[41−45]

Hence, to examine the structures of $UO_2(hfacac)_2DMSO$ in o-$C_6D_4Cl_2$ and sc-CO_2 containing free Hhfacac, we measured ^1H and ^{19}F NMR spectra of o-$C_6D_4Cl_2$ and sc-CO_2 containing $UO_2(hfacac)_2DMSO$ (1.01×10^{-2}, 1.03×10^{-2} M) and free Hhfacac (2.83×10^{-2}, 2.96×10^{-2} M),
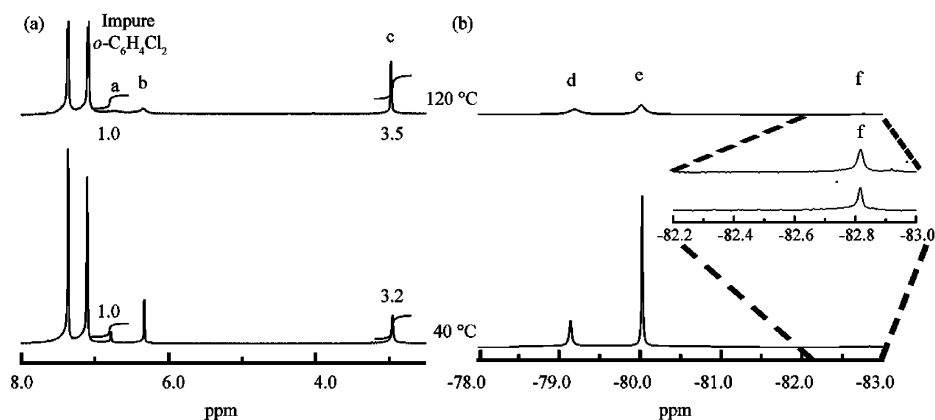
(59) Mizuguchi, K.; Lee, S.-H.; Ikeda, Y.; Tomiyasu, H. *J. Alloys Compd.* **1998**, *271−273*, 163−167.

(60) Kayaki, Y.; Suzuki, T.; Noguchi, Y.; Sakurai, S.; Imanari, M.; Ikariya, T. *Chem. Lett.* **2002**, *31*, 424−425.
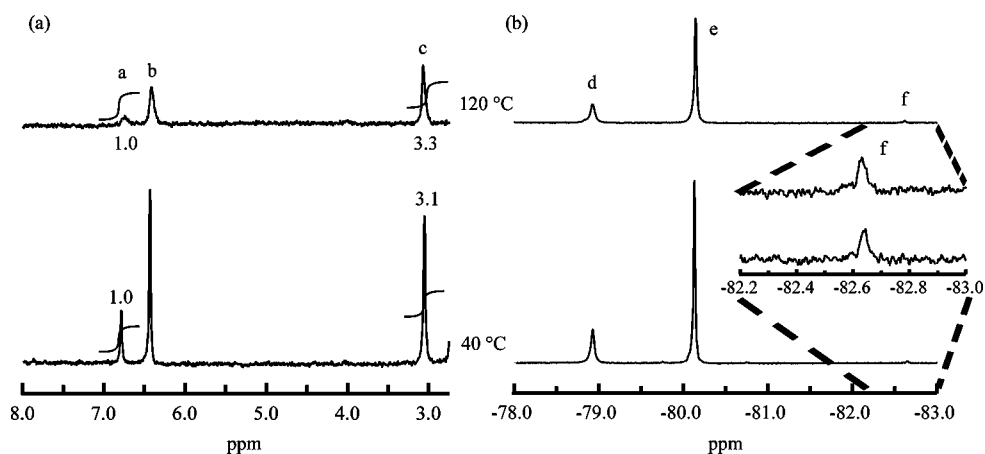
(61) Binsch, G. *Top. Stereochem.* **1968**, *3*, 97−192.

(62) Budzelaar, P. H. M. *gNMR*, version 5.0; Adept Scientific.

(63) Li, H.; Ji, X.; Yan, J. *Int. J. Energy Res.* **2006**, *30*, 135−148.

Figure 1. ^{1}H (a) and ^{19}F (b) NMR spectra of o-$C_6D_4Cl_2$ containing $UO_2(hfacac)_2DMSO$ (1.01×10^{-2} M) and free Hhfacac (2.83×10^{-2} M) at 40 and 120 °C.

Figure 2. ^{1}H (a) and ^{19}F (b) NMR spectra of sc-CO_2 containing $UO_2(hfacac)_2DMSO$ (1.03×10^{-2} M) and free Hhfacac (2.96×10^{-2} M) at 40 and 120 °C.

respectively. The results are shown in Figures 1 and 2. Signals a, b, and c in part (a) in Figure 1 and part (a) in Figure 2 are assigned as the −CH groups of coordinated hfacac and free Henol and the −CH$_3$ group of coordinated DMSO, respectively. The −CH$_2$ group due to free Keto could not be observed in both systems, because the amount of Keto is small in the present samples. Signals d, e, and f in part (b) of Figure 1 and part (b) of Figure 2 correspond to the −CF$_3$ groups of coordinated hfacac, and those of free Henol and Keto, respectively. From the area ratios of signals b and c to a and of signal e to d at 40 °C, it was found that two hfacac and one DMSO coordinate to the uranyl ion. The chemical shifts of signals b and c were found to be constant regardless of an increase in temperature. These results indicate that even in the o-$C_6D_4Cl_2$ and sc-CO_2 systems containing free Hhfacac the $UO_2(hfacac)_2DMSO$ complex maintains the pentagonal bipyramidal structure and that the following equilibrium does not exist in both systems:

$$UO_2(hfacac)_2DMSO + Hhfacac$$
$$= UO_2(hfacac)_2Hhfacac + DMSO \quad (3)$$
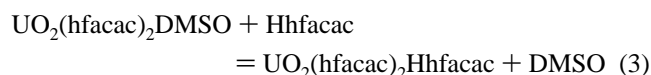
Moreover, the chemical shift differences ($\Delta\delta$) between signals a and b, and signals d and e are 0.45 and 1.25 ppm for the o-$C_6D_4Cl_2$ system, and 0.32 and 1.09 ppm for the sc-CO_2 system (Figures S2 and S3 in the Supporting Information). The $\Delta\delta$ values in the o-$C_6D_4Cl_2$ system are larger than those in sc-CO_2. This suggests that hfacac of $UO_2(hfacac)_2DMSO$ in the o-$C_6D_4Cl_2$ coordinates to the uranyl ion more strongly than that in sc-CO_2.

From NMR results, it is expected that the U=O bond strength of $UO_2(hfacac)_2DMSO$ in o-$C_6H_4Cl_2$ is weaker than that of $UO_2(hfacac)_2DMSO$ in sc-CO_2, and hence the U=O stretching band of $UO_2(hfacac)_2DMSO$ in o-$C_6H_4Cl_2$ should be observed at a lower wavenumber than that in sc-CO_2. In fact, the U=O symmetric stretching (ν_1) bands of $UO_2(hfacac)_2$-DMSO (1.0×10^{-2} M) in o-$C_6H_4Cl_2$ and sc-CO_2 were observed at 854 ± 1 and 859 ± 1 cm^{-1}, respectively (Figure S4 in the Supporting Information). To confirm the significance of the difference ($\Delta\nu_1$, 5 cm^{-1}) in the ν_1 bands of $UO_2(hfacac)_2DMSO$ in o-$C_6H_4Cl_2$ and sc-CO_2, we measured the Raman spectra of $UO_2(acac)_2DMSO$ and $UO_2(acac)_2$-DMF in o-$C_6H_4Cl_2$. The ν_1 bands of $UO_2(acac)_2DMSO$ and $UO_2(acac)_2DMF$ were observed at 830 ± 1 and 834 ± 1 cm^{-1}, respectively (Figure S4 in the Supporting Information). The $\Delta\nu_1$ value of 4 cm^{-1} should reflect the difference in the donicity of DMSO and DMF, that is, DMSO coordinates to the uranyl ion more strongly than DMF. In addition, the $\Delta\nu_1$ value between $UO_2(hfacac)_2DMSO$ (854 cm^{-1}) and $UO_2(acac)_2$-DMSO (830 cm^{-1}) in o-$C_6H_4Cl_2$ is 24 cm^{-1}, which also reflects the difference in the strength of the coordination of

Table 1. Solution Compositions and Kinetic Parameters for the Exchange Reactions of hfacac in $UO_2(hfacac)_2DMSO$ in $o\text{-}C_6D_4Cl_2$ (i − xii) and sc-CO_2 (I− XII)

solution number	[UO$_2$(hfacac)$_2$DMSO] 10^{-2} M	[Henol] 10^{-2} M	[DMSO] 10^{-3} M	k_{hf} (80 °C) s^{-1}	$\Delta H^{\ddagger}$ kJ·mol^{-1}	$\Delta S^{\ddagger}$ J·mol^{-1}·K^{-1}
i	1.08	0.623	0	8.35	46.4 ± 2.1	−95.8 ± 5.5
ii	1.08	1.63	0	18.8	41.3 ± 1.8	−106 ± 5
iii	1.05	2.31	0	23.4	44.3 ± 1.4	−98.5 ± 3.7
iv	1.01	2.83	0	27.2	42.3 ± 1.7	−99.1 ± 4.8
v	1.05	4.31	0	43.7	41.7 ± 1.8	−98.6 ± 5.9
vi	1.05	5.36	0	48.0	37.0 ± 1.4	−110 ± 4
vii	1.05	8.77	0	64.3	36.3 ± 1.0	−109 ± 3
viii	1.01	2.83	0	27.2	42.3 ± 1.7	−99.1 ± 4.8
ix	1.01	2.83	5.01	21.3	44.3 ± 1.4	−96.8 ± 7.5
x	1.01	2.83	10.6	24.1	44.5 ± 2.7	−95.4 ± 7.6
xi	1.01	2.83	14.8	18.2	49.8 ± 2.2	−82.1 ± 6.3
xii	1.01	2.83	19.9	17.2	46.7 ± 2.7	−90.5 ± 7.3
I	1.03	0.907	0	4.84	25.3 ± 0.7	−162 ± 2
II	1.06	1.98	0	8.58	24.6 ± 0.8	−159 ± 3
III	1.03	2.96	0	10.4	27.8 ± 0.9	−148 ± 2
IV	1.03	4.09	0	13.4	25.5 ± 1.0	−154 ± 3
V	1.03	4.66	0	17.9	23.8 ± 1.2	−156 ± 3
VI	0.989	5.62	0	22.9	24.0 ± 1.8	−153 ± 5
VII	0.972	7.50	0	28.7	22.2 ± 0.8	−157 ± 2
VIII	1.01	2.96	0	10.4	27.8 ± 0.9	−148 ± 2
IX	0.989	2.94	2.01	8.81	27.6 ± 1.3	−150 ± 4
X	1.00	2.89	4.78	7.84	26.0 ± 1.8	−154 ± 5
XI	1.03	2.78	6.97	7.00	27.2 ± 1.7	−152 ± 5
XII	0.989	2.80	9.67	7.00	26.5 ± 1.5	−154 ± 4

acac and hfacac. These results are consistent with previous studies that the ν_1 bands of the uranyl complexes shift toward a lower wavenumber with an increase in the donicity (strength of coordination) of ligands coordinated to the equatorial plane of the uranyl moiety.[64,65]

From the results of NMR and Raman spectra, it is concluded that the hfacac of $UO_2(hfacac)_2DMSO$ in $o\text{-}C_6D_4\text{-}Cl_2$ coordinates to the uranyl ion more strongly than that in sc-CO_2.

Exchange Reactions between Free Hhfacac and Coordinated hfacac in $UO_2(hfacac)_2DMSO$ in $o\text{-}C_6D_4Cl_2$ and sc-CO_2. As seen in Figures 1 and 2, the signals of the −CH group (a and b) and the −CF$_3$ group (d and e) for coordinated hfacac and free Hhfacac become broad with increasing temperature, whereas the signal of −CF$_3$ group (f) for Keto does not show such a broadening. From the similarity to the NMR spectral changes of $UO_2(acac)_2L$ (L = DMSO, DMF) in $o\text{-}C_6D_4Cl_2$,[50,52] it was found that Henol exchanges with the coordinated hfacac in $UO_2(hfacac)_2DMSO$ in $o\text{-}C_6D_4\text{-}Cl_2$ and sc-CO_2 as follows:

$$UO_2(hfacac)_2DMSO + Henol^* =$$
$$UO_2(hfacac)(hfacac^*)DMSO + Henol \quad (4)$$
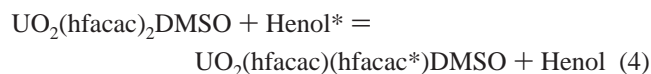
where the asterisk denotes the exchanging species.

Hence, we measured signals d and e of the same samples as those in Figures 1 and 2 at various temperatures to obtain kinetic data (Figure S5 in the Supporting Information).

The apparent first-order rate constants (k_{hf}) for the hfacac exchange reaction in $UO_2(hfacac)_2DMSO$ were evaluated

(64) Zazhogin, A. A.; Lutz, H. D.; Komyak, A. I. *J. Mol. Struct.* **1999**, *482−483*, 189−193.
(65) Koshino, N.; Harada, M.; Nogami, M.; Morita, Y.; Kikuchi, T.; Ikeda, Y. *Inorg. Chim. Acta* **2005**, *358*, 1857−1864.

from the τ-values using eq 1. It was also confirmed that the k_{hf} values evaluated using the signals of the −CH group (a and b) are almost same as those using the −CF$_3$ group (d and e). The k_{hf} values for the samples (i−vii) and (I−VII) listed in Table 1 were measured, and their logarithmic values were plotted against the reciprocal temperature in Figure 3. The k_{hf} values in sc-CO_2 are found to be smaller than those in $o\text{-}C_6D_4Cl_2$. However, pressure in $o\text{-}C_6D_4Cl_2$ the system differs from that in the sc-CO_2 system. Hence, the k_{hf} values in the $o\text{-}C_6D_4Cl_2$ system (sample vi in Table 1) were measured at various temperatures under atmospheric pressure and 25 MPa. The k_{hf} values at 25 MPa were found to be almost the same as those at atmospheric pressure (Figure S6 in the Supporting Information). This indicates that the differences in k_{hf} values between $o\text{-}C_6D_4Cl_2$ and sc-CO_2 systems are due to those in the solvents.
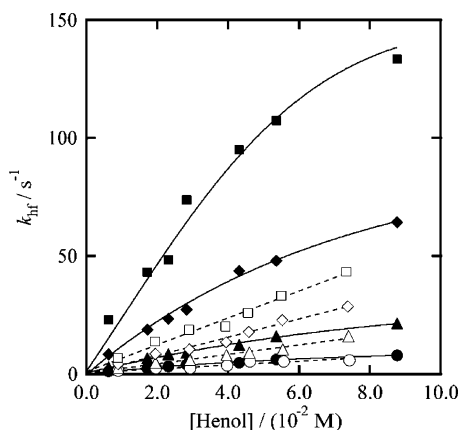
Furthermore, it is found from Figure 3 that the k_{hf} values increase with increasing [Henol] in both systems. Hence, the
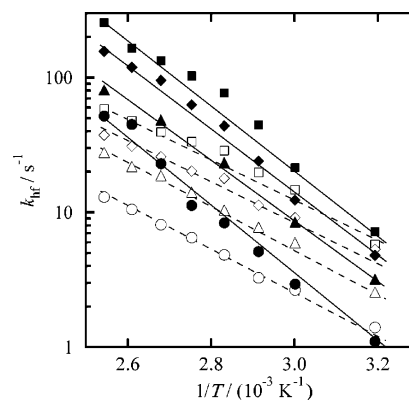

Figure 3. Semilogarithmic plots of k_{hf} versus $1/T$ for the exchange reactions of hfacac in $UO_2(hfacac)_2DMSO$ in $o\text{-}C_6D_4Cl_2$ and sc-CO_2. The symbols of ●, ▲, ◆, ■, ○, △, ◇, and □ correspond to data for solutions (i, iii, iv, vii ,I, III, IV, and VII) in Table 1.

Figure 4. Plots of k_{hf} versus [Henol] for the exchange reactions of hfacac in $UO_2(hfacac)_2DMSO$. (a): (●) 40 °C, (▲) 60 °C, (◆) 80 °C, (■) 100 °C in the o-$C_6D_4Cl_2$ system. (b): (○) 40 °C, (△) 60 °C, (◇) 80 °C, (□) 100 °C in the sc-CO_2 system.
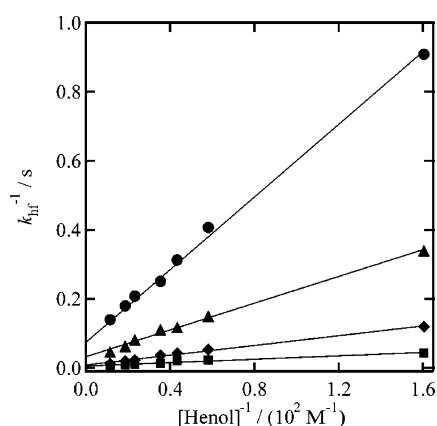
Figure 5. Plots of k_{hf}^{-1} versus [Henol]$^{-1}$ for the exchange reactions of hfacac in $UO_2(hfacac)_2DMSO$ in o-$C_6D_4Cl_2$. (●) 40 °C, (▲) 60 °C, (◆) 80 °C, (■) 100 °C.

Table 2. Values of k_a, k_b, k_m, and k_n in the o-$C_6D_4Cl_2$ System at Various Temperatures

Temperature	k_a	k_b	k_m	k_n
°C	10^{-3} s	10^{-4} M·s	10^{-2} s	10^{-1} M·s
40	72.9 ± 10.4	55.9 ± 0.3	23.4 ± 5.6	233 ± 46
60	27.9 ± 3.1	27.3 ± 0.6	11.5 ± 0.4	75.7 ± 3.4
70	16.3 ± 1.5	11.2 ± 0.3	6.89 ± 0.26	25.0 ± 2.1
80	8.33 ± 1.77	6.99 ± 0.27	3.75 ± 0.38	10.1 ± 3.1
90	4.23 ± 1.25	4.88 ± 0.70	2.21 ± 0.18	5.27 ± 1.48
100	2.91 ± 1.28	3.06 ± 0.47	1.37 ± 0.05	4.94 ± 0.37

k_{hf} values were plotted against [Henol] as shown in Figure 4. The k_{hf} values for the o-$C_6D_4Cl_2$ system are found to approach constant values with an increase in [Henol]. This result is consistent with the exchange reaction of acac in $UO_2(acac)_2L$ in o-$C_6H_4Cl_2$.[50,52] Plots of $1/k_{hf}$ versus [Henol] give straight lines with intercepts (Figure 5) and result in the following equation:

$$1/k_{hf} = k_a + k_b[\text{Henol}]^{-1} \tag{5}$$

The values of k_a and k_b were obtained from the intercepts and the slopes in Figure 5, respectively, and are listed in Table 2.
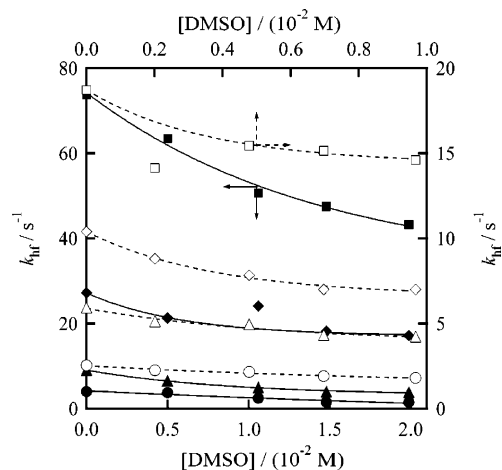
Figure 6. Plots of k_{hf} versus [DMSO] for the exchange reactions of hfacac in $UO_2(hfacac)_2DMSO$. (a): (●) 40 °C, (▲) 60 °C, (◆) 80 °C, (■) 100 °C in the o-$C_6D_4Cl_2$ system. (b): (○) 40 °C, (△) 60 °C, (◇) 80 °C, (□) 100 °C in the sc-CO_2 system.

Table 3. Values of k_c, k_o, and k_p in sc-CO_2 System at Various Temperatures

| Temperature	k_c	k_o	k_p
°C	10^2 M^{-1}·s^{-1}	10^{-2} s	M·s
40	0.915 ± 0.055	38.3 ± 1.5	13.0 ± 2.51
60	1.97 ± 0.04	17.9 ± 0.7	6.53 ± 1.28
70	2.60 ± 0.07	13.6 ± 0.8	6.71 ± 1.46
80	3.83 ± 0.09	9.24 ± 0.56	3.42 ± 0.93
90	4.68 ± 0.14	7.53 ± 0.76	1.29 ± 0.13
100	5.72 ± 0.16	6.17 ± 0.48	0.991 ± 0.082

On the other hand, in the sc-CO_2 system, the plots of k_{hf} versus [Henol] give straight lines as shown in Figure 4, that is, the following equation can be derived:

$$k_{hf} = k_c[\text{Henol}] \tag{6}$$

The k_c values were obtained from the slopes in Figure 4 and are listed in Table 3.

From these results, it is clear that there is difference in the exchange reactions of hfacac in $UO_2(hfacac)_2DMSO$ in o-$C_6D_4Cl_2$ and sc-CO_2 systems, as will be described later in the proposed mechanisms.

Effect of Added DMSO on the Exchange Rates of hfacac in o-$C_6D_4Cl_2$ and sc-CO_2. It has been known that the coordinated DMSO in $UO_2(\beta$-diketonato)$_2$DMSO (β-diketonates = acac, dbm, hfacac) rapidly exchanges with free DMSO at room temperature[41,47,49] and that the LA−LB interactions exist between DMSO and CO_2 in sc-CO_2.[31,32] Considering these facts, the exchange reaction of hfacac in the present study should be affected by the free DMSO. To examine the effect of free DMSO on the hfacac exchange reactions in $UO_2(hfacac)_2DMSO$ in o-$C_6D_4Cl_2$ and sc-CO_2, the kinetic experiments were carried out using the sample solutions (viii−xii and VIII−XII) listed in Table 1. The resulting k_{hf} values were plotted against [DMSO] in Figure 6. As seen from this figure, the k_{hf} values become small, with an increase in [DMSO], and the average reduction ratio (33.3%) of k_{hf} values in the o-$C_6D_4Cl_2$ system is smaller than that (25.6%) in sc-CO_2. This result suggests that the effect of free DMSO on the exchange reaction of hfacac in
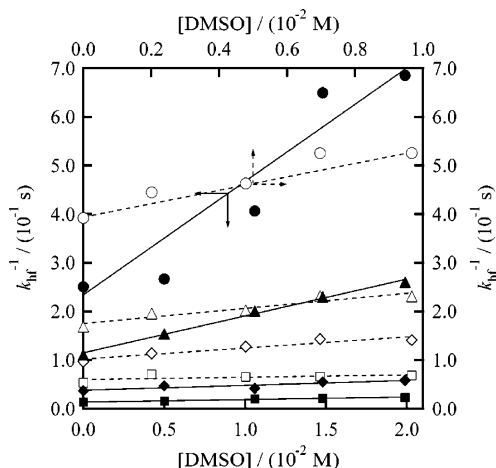
Figure 7. Plots of $1/k_{hf}$ versus [DMSO] for the exchange reactions of hfacac in $UO_2(hfacac)_2DMSO$. (a): (●) 40 °C, (▲) 60 °C, (◆) 80 °C, (■) 100 °C in the o-$C_6D_4Cl_2$ system. (b): (○) 40 °C, (△) 60 °C, (◇) 80 °C, (□) 100 °C in the sc-CO_2 system.
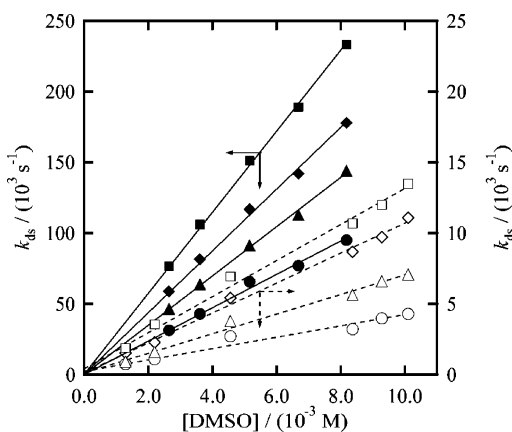
Figure 8. Plots of k_{ds} versus [DMSO] for the exchange reactions of DMSO in $UO_2(hfacac)_2DMSO$. (a): (●) 40 °C, (▲) 60 °C, (◆) 80 °C, (■) 100 °C in the o-$C_6D_4Cl_2$ system. (b): (○) 40 °C, (△) 60 °C, (◇) 80 °C, (□) 100 °C in the sc-CO_2 system.

$UO_2(hfacac)_2DMSO$ in the sc-CO_2 system is depressed by sc-CO_2 and that the LA–LB interaction between CO_2 and DMSO affects the ligand exchange reaction in $UO_2(hfacac)_2$-DMSO. However, the $\Delta H^{\ddagger}$ values for k_{hf} in the presence of free DMSO are almost the same as those in the absence of free DMSO (Table 1). This suggests that the rate-determining step in the hfacac exchange should be same regardless of

the presence of free DMSO. The plots of the $1/k_{hf}$ values against [DMSO] for the o-$C_6D_4Cl_2$ and sc-CO_2 systems give straight lines with intercepts as shown in Figure 7. These results give the following equations.

$$1/k_{hf} = k_m + k_n[DMSO] \text{ (for the } o\text{-}C_6D_4Cl_2 \text{ system) (7)}$$

$$1/k_{hf} = k_o + k_p[DMSO] \text{ (for the sc-}CO_2 \text{ system) (8)}$$

The values of k_m, k_n, k_o, and k_p were obtained from the intercepts and slopes in Figure 7 and are listed in Tables 2 and 3.

Exchange Reactions between Free DMSO and Coordinated DMSO in $UO_2(hfacac)_2DMSO$ in o-$C_6D_4Cl_2$ and sc-CO_2. To examine the effect of free DMSO on the exchange reaction of hfacac in $UO_2(hfacac)_2DMSO$ in o-$C_6D_4Cl_2$ and sc-CO_2 in more detail, the kinetic studies on the DMSO exchange reactions between free and coordinated sites in $UO_2(hfacac)_2DMSO$ in both systems were carried out using sample solutions (xiii−xvii, XIII−XVIII) listed in Table 4. In the temperature region of 40 to 100 °C, one peak corresponding to the −CH₃ proton signal of DMSO was observed in both systems (see the left side of Figures S7 and S8 in the Supporting Information). These results are consistent with the phenomena observed in DMSO exchanges in $UO_2(\beta\text{-diketonato})_2DMSO$ (β-diketonates = acac, dbm, hfacac) in CD_2Cl_2,[41,47,49] indicating that in this temperature range the free DMSO exchanges very rapidly with the coordinated DMSO in $UO_2(hfacac)_2DMSO$ in o-$C_6D_4Cl_2$ and sc-CO_2. However, the coalescence signals of the −CH₃ group in the sc-CO_2 system become broad with an increase in the temperature in spite of the rapid exchange region (Figure S8 in the Supporting Information). This is due to the lowering of the NMR resolution as mentioned in Experimental Section. In fact, the −CH₃ (−CF₃) signals of the ligands in sc-CO_2 containing only $UO_2(hfacac)_2DMSO$ or ligands also become broad with increasing temperature (Figure S9 in the Supporting Information). By considering these results, we carried out the line shape analyses of NMR spectra in Figures S7 and S8 to obtain kinetic data. The apparent first-order rate constants (k_{ds}) for the DMSO exchange reactions in $UO_2(hfacac)_2DMSO$ in o-$C_6D_4Cl_2$ and sc-CO_2 were plotted

Table 4. Solution Compositions and Kinetic Parameters for the Exchange Reactions of DMSO in $UO_2(hfacac)_2DMSO$ in o-$C_6D_4Cl_2$ (xiii − xvii) and sc-CO_2 (XIII− XVIII)

Solution Number	$[UO_2(hfacac)_2DMSO]$	[DMSO]	k_{ds} (80 °C)	$\Delta H^{\ddagger}$	$\Delta S^{\ddagger}$
	10^{-2} M	10^{-3} M	s^{-1}	kJ·mol^{-1}	J·mol^{-1}·K^{-1}
xiii	1.01	2.65	5.89×10^4	11.5 ± 0.2	-122 ± 1
xiv	1.05	3.61	8.15×10^4	11.8 ± 0.8	-119 ± 1
xv	1.05	5.16	1.17×10^5	10.4 ± 0.4	-120 ± 2
xvi	1.05	6.68	1.42×10^5	11.3 ± 0.4	-116 ± 3
xvii	1.08	8.81	1.78×10^5	10.6 ± 0.6	-115 ± 2
XIII	1.07	1.29	1.54×10^3	17.8 ± 0.8	-131 ± 3
XIV	1.07	2.20	2.29×10^3	15.6 ± 0.7	-142 ± 2
XV	1.07	4.56	5.43×10^3	12.0 ± 0.7	-141 ± 4
XVI	1.04	8.37	8.67×10^3	15.5 ± 0.9	-128 ± 2
XVII	1.07	9.28	9.72×10^3	14.8 ± 0.8	-129 ± 2
XVIII	1.04	10.1	11.1×10^3	16.3 ± 0.8	-123 ± 2

Scheme 1
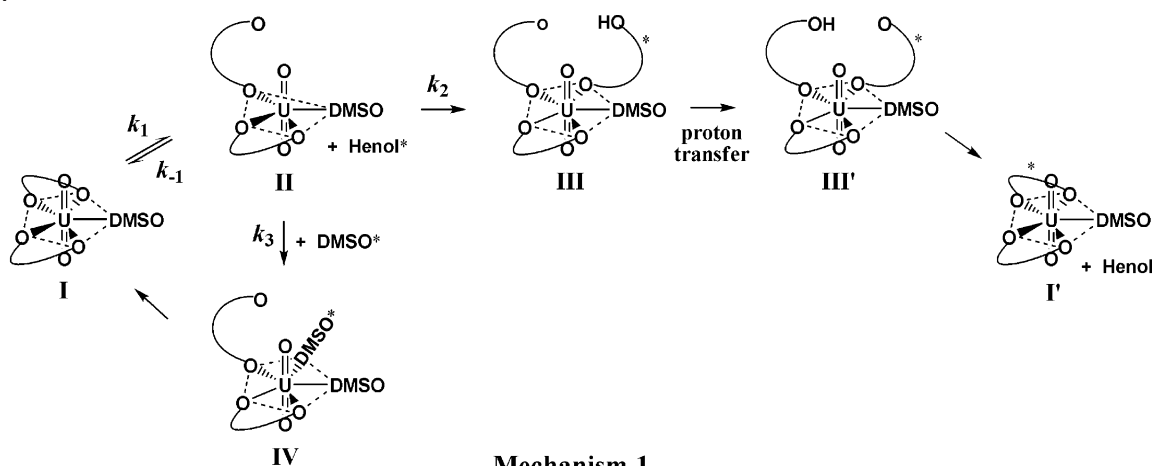
Mechanism 1
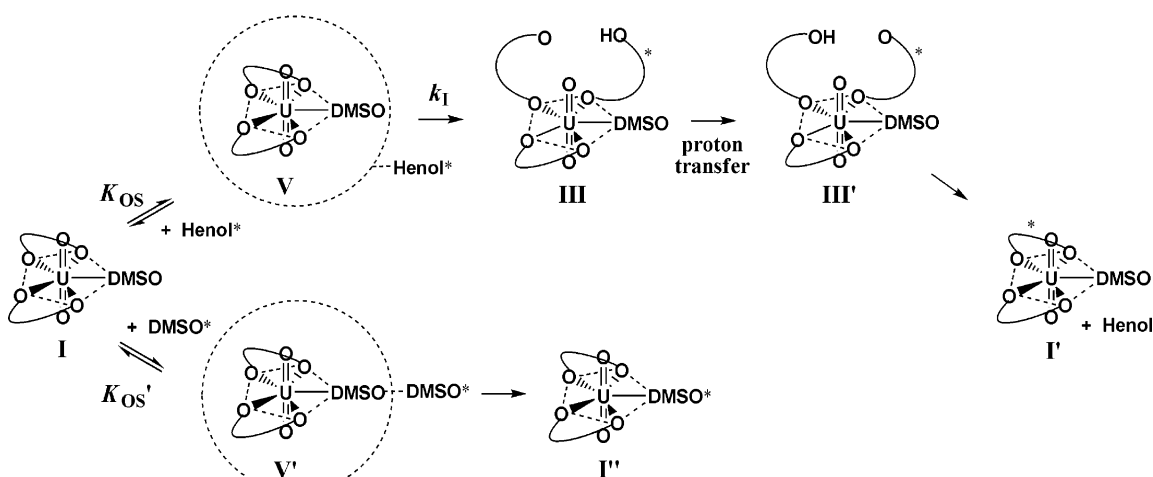
Mechanism 2

Table 5. Values of k_y and k_z at Various Temperatures and Kinetic Parameters in the o-C$_6$D$_4$Cl$_2$ and sc-CO$_2$ Systems

	Temperature/°C	40	60	70	80	90	100
o-C$_6$D$_4$Cl$_2$	$k_y/10^7$ M$^{-1}\cdot$s^{-1}	1.18 ± 0.02	1.74 ± 0.02	1.93 ± 0.02	2.19 ± 0.03	2.51 ± 0.02	2.87 ± 0.02
			$\Delta H^{\ddagger} = 11.2 \pm 0.5$ kJ$\cdot$mol^{-1}, $\Delta S^{\ddagger} = -74.1 \pm 1.6$ J$\cdot$mol$^{-1}\cdot$K^{-1}					
sc-CO$_2$	$k_z/10^5$ M$^{-1}\cdot$s^{-1}	4.31 ± 0.23	7.08 ± 0.17	8.74 ± 0.14	10.7 ± 0.2	11.9 ± 0.21	13.3 ± 0.3
			$\Delta H^{\ddagger} = 13.4 \pm 1.1$ kJ$\cdot$mol^{-1}, $\Delta S^{\ddagger} = -93.5 \pm 3.2$ J$\cdot$mol$^{-1}\cdot$K^{-1}					

against [DMSO] as shown in Figure 8. From this figure, the following equations can be derived.

$$k_{ds} = k_y[\text{DMSO}] \text{ (for the } o\text{-C}_6\text{D}_4\text{Cl}_2 \text{ system)} \quad (9)$$

$$k_{ds} = k_z[\text{DMSO}] \text{ (for the sc-CO}_2 \text{ system)} \quad (10)$$

These results suggest that the DMSO exchange reactions in UO$_2$(hfacac)$_2$DMSO in both systems proceed associatively. The k_y and k_z values obtained from the slopes in Figure 8 are listed in Table 5. The values of k_z are fairly smaller than those of k_y. This difference must be due to that the associative approach of free DMSO to UO$_2$(hfacac)$_2$DMSO is hindered by the formation of the LA−LB interaction between free DMSO and sc-CO$_2$.

Mechanism. The exchange reactions of hfacac in UO$_2$(hfacac)$_2$DMSO in o-C$_6$D$_4$Cl$_2$ and sc-CO$_2$ depend on

[Henol] as shown in Figures 4. This suggests that the hfacac exchange reactions in UO$_2$(hfacac)$_2$DMSO proceed associatively. However, the associative (A) mechanism[66] should be ruled out in both systems, because in the o-C$_6$D$_4$Cl$_2$ system the k_{hf} values for the hfacac exchange reaction do not increase linearly but asymptoticically with increasing [Henol], and in the o-C$_6$D$_4$Cl$_2$ and sc-CO$_2$ systems the k_{hf} values do not decrease linearly with an increase in [DMSO] as shown in Figure 6.

Considering the similarity to the acac exchange reactions in UO$_2$(acac)$_2$L (L = DMSO, DMF),[50,52] two mechanisms shown in Scheme 1 should be proposed. In Mechanism 1 (I → II → III → III′ → I′), k_{hf} is expressed as follows.

(66) Langford, C. H.; Gray, H. B. *Ligand Substitution Processes*; W. A. Benjamin: New York, 1966.

$$k_{hf} = k_1 k_2 [\text{Henol}]/(k_{-1} + k_2 [\text{Henol}]) \qquad (11)$$

$$1/k_{hf} = 1/k_1 + k_{-1}/(k_1 k_2)[\text{Henol}]^{-1} \qquad (12)$$

Eq 12 is consistent with eq 5 for the o-$C_6D_4Cl_2$ system, and hence k_a and k_b are related as follows:

$$k_a = 1/k_1, \quad k_b = k_{-1}/(k_1 k_2) \qquad (13)$$

In the sc-CO_2 system, it is expected that the ring closure of unidentate hfacac in the II → I pathway occurs more rapidly than the coordination of the incoming Henol* (II → III), because of difficulty in the approach of the relatively bulky Henol* to intermediate II through the existence of the LA−LB interaction and hydrogen bonding between Henol and CO_2.[31,32] Thus, the condition $k_{-1} \gg k_2[\text{Henol}]$ should hold under the experimental conditions in the sc-CO_2 system, and the following eq 14 can be derived from eq 11.

$$k_{hf} = (k_1 k_2/k_{-1})[\text{Henol}] \qquad (14)$$

Eq 14 is consistent with eq 6, and hence k_c is related as follows:

$$k_c = k_1 k_2/k_{-1} \qquad (15)$$

In Mechanism 2 (I → V → III → III′ → I′), V is an outer-sphere complex and K_{OS} is the outer-sphere complex formation constant. In this mechanism, k_{hf} is given by eq 16.[50,52]

$$k_{hf} = k_I K_{OS}[\text{Henol}]/(1 + K_{OS}[\text{Henol}]) \qquad (16)$$

$$1/k_{hf} = 1/k_I + 1/(k_I K_{OS})[\text{Henol}]^{-1} \qquad (17)$$

Eq 17 is also consistent with eq 5. Hence, the following relationships are obtained.

$$k_a = 1/k_I, \quad k_b = 1/(k_I K_{OS}) \qquad (18)$$

If the condition, $K_{OS}[\text{Henol}] \ll 1$, holds in the sc-$CO_2$ system, the following equation can be derived and is consistent with eq 6.

$$k_{hf} = k_I K_{OS}[\text{Henol}] \qquad (19)$$

It is likely that the values of $K_{OS}[\text{Henol}]$ are less than 1 in the sc-CO_2 system because $UO_2(hfacac)_2DMSO$ and Henol are noncharged species, [Henol] in the present study is in the range from 9.07×10^{-3} to 7.50×10^{-2} M, and the approach of Henol to $UO_2(hfacac)_2DMSO$ should be inhibited by the intermolecular interactions between Henol and CO_2.[31,32] Thus, k_c is related as follows:

$$k_c = k_I K_{OS} \qquad (20)$$

Furthermore, the DMSO exchange reactions in $UO_2(hfacac)_2DMSO$ in o-$C_6D_4Cl_2$ and sc-CO_2 systems proceed associatively. Hence, it is expected that the free DMSO participates in the hfacac exchange reaction in $UO_2(hfacac)_2DMSO$ as shown in Scheme 1. In Mechanism 1, DMSO* competes with Henol* in the coordination to the vacant site of intermediate II. In this mechanism, k_{hf} is expressed as follows:

$$k_{hf} = k_1 k_2 [\text{Henol}]/(k_{-1} + k_2 [\text{Henol}] + k_3 [\text{DMSO}]) \qquad (21)$$

$$1/k_{hf} = (k_{-1} + k_2 [\text{Henol}])/(k_1 k_2 [\text{Henol}]) + \\ k_3/(k_1 k_2 [\text{Henol}])[\text{DMSO}] \qquad (22)$$

On the other hand, in Mechanism 2, DMSO* forms an outer-sphere complex (V′) with $UO_2(hfacac)_2DMSO$. From this mechanism, the following equations are derived.

$$k_{hf} = k_I K_{OS}[\text{Henol}]/(1 + K_{OS}[\text{Henol}] + K_{OS}'[\text{DMSO}]) \qquad (23)$$

$$1/k_{hf} = (1 + K_{OS}[\text{Henol}])/(k_I K_{OS}[\text{Henol}]) + \\ K_{OS}'/(k_I K_{OS}[\text{Henol}])[\text{DMSO}] \qquad (24)$$

It is apparent that eqs 22 and 24 are correlated with eqs 7 and 8 as follows.

$$k_m = k_o = (k_{-1} + k_2 [\text{Henol}])/(k_1 k_2 [\text{Henol}]), \\ k_n = k_p = k_3/(k_1 k_2 [\text{Henol}]) \qquad (25)$$

$$k_m = k_o = (1 + K_{OS}[\text{Henol}])/(k_I K_{OS}[\text{Henol}]), \\ k_n = k_p = K_{OS}'/(k_I K_{OS}[\text{Henol}]) \qquad (26)$$

From eqs 13, 15, 18, and 20, the relations of $k_1 = k_I$ and $k_2/k_{-1} = K_{OS}$ can be derived. The values of k_1 or k_I, k_2/k_{-1} or K_{OS}, k_3/k_2, and K_{OS}' in o-$C_6D_4Cl_2$ and sc-CO_2 systems were calculated from the values (k_a, k_b, k_m, k_n, k_c, k_o, and k_p) in Tables 2 and 3 and the average value (2.87×10^{-2} and 2.83×10^{-2} M) of [Henol] in solutions viii−xii and VIII− XII, respectively. The results are listed in Tables 6 and 7 with the activation parameters for k_1 or k_I in o-$C_6D_4Cl_2$ and sc-CO_2 systems.

As seen from Tables 6 and 7, the K_{os} values in sc-CO_2 system are less than 1. This result supports that the condition of $K_{OS}[\text{Henol}] \ll 1$ in Mechanism 2 holds in sc-CO_2 system. However, the K_{OS}' values in o-$C_6D_4Cl_2$ and sc-CO_2 systems are much larger than the value (0.86 M^{-1}) expected from the Fuoss−Eigen equation[67] (for an interaction distance of 7 Å) and the value (4.9 M^{-1} at 25 °C) obtained for the DMSO exchange in the $UO_2(acac)_2DMSO$ in CD_2Cl_2.[47]

Therefore, it is proposed that the exchange reactions of hfacac in $UO_2(hfacac)_2DMSO$ in o-$C_6D_4Cl_2$ and sc-CO_2 proceed through Mechanism 1.

Comparisons of Kinetic Parameters for o-$C_6D_4Cl_2$ and sc-CO_2 Systems. On the basis of Mechanism 1, we discuss the differences in the kinetic parameters for the exchange reactions of hfacac in $UO_2(hfacac)_2DMSO$ in the o-$C_6D_4Cl_2$ and sc-CO_2 systems. The k_1 values in the o-$C_6D_4Cl_2$ system are smaller than those in sc-CO_2 (Tables 6 and 7). This suggests that the ring-opening of coordinated hfacac in $UO_2(hfacac)_2DMSO$ takes place more easily in sc-CO_2 than in o-$C_6D_4Cl_2$, that is, the hfacac ligand of $UO_2(hfacac)_2$-DMSO in sc-CO_2 coordinates to the uranyl moiety more weakly than in o-$C_6D_4Cl_2$. This consideration is supported by the results of structural experiments using NMR and Raman spectrometers (Figures S2−S4 in the Supporting Information), and the fact that the $\Delta H^{\ddagger}$ value for k_1 in sc-CO_2 system is smaller than that in o-$C_6D_4Cl_2$. Furthermore,

---

(67) Fuoss, R. M. *J. Am. Chem. Soc.* **1958**, *80*, 5059−5061.

Table 6. Values of k_1 or k_I, k_2/k_{-1} or K_{OS}, k_3/k_2, and K_{OS}' at Various Temperatures and Kinetic Parameters for k_1 or k_I and k_3 Pathways in the o-C$_6$D$_4$Cl$_2$ System[a]

Temperature	k_1 or k_I	k_2/k_{-1} or K_{OS}		K_{OS}'
°C	s^{-1}	M^{-1}	k_3/k_2	M^{-1}
40	13.7 ± 1.9	14.1 ± 3.0	9.16 ± 0.61	120 ± 26
60	35.8 ± 3.2	10.2 ± 1.6	7.78 ± 0.70	79.4 ± 10.1
70	61.3 ± 5.5	14.6 ± 1.3	4.40 ± 0.95	64.1 ± 8.0
80	120 ± 23	11.9 ± 2.3	3.48 ± 1.48	41.5 ± 12.7
90	236 ± 70	8.67 ± 2.6	2.58 ± 1.49	31.0 ± 8.7
100	344 ± 151	9.51 ± 4.2	3.87 ± 1.60	46.3 ± 3.5

[a] Kinetic parameters for k_1 or k_I: $\Delta H^{\ddagger} = 57.8 \pm 2.7$ kJ·mol^{-1}, $\Delta S^{\ddagger} = -42.9 \pm 7.7$ J·mol^{-1}·K^{-1}.

Table 7. Values of k_1 or k_I, k_2/k_{-1} or K_{OS}, k_3/k_2, and K_{OS}' at Various Temperatures and Kinetic Parameters for k_1 or k_I and k_3 Pathways in sc-CO$_2$ System[a]

Temperature	k_1 or k_I	k_2/k_{-1} or k_{OS}		K_{OS}'
°C	10^2 s^{-1}	M^{-1}	k_3/k_2	M^{-1}
40	2.33 ± 0.56	0.393 ± 0.088	86.8 ± 26.8	34.1 ± 7.0
60	5.18 ± 0.50	0.380 ± 0.036	97.1 ± 21.2	36.9 ± 7.3
70	6.18 ± 0.74	0.422 ± 0.049	119 ± 30	50.2 ± 11.0
80	7.61 ± 0.75	0.503 ± 0.048	74.7 ± 21.6	37.6 ± 10.3
90	11.6 ± 1.72	0.404 ± 0.059	41.9 ± 7.7	15.7 ± 1.8
100	15.9 ± 1.76	0.348 ± 0.053	44.2 ± 37.0	17.3 ± 13.5

[a] Kinetic parameters for k_1 or k_I: $\Delta H^{\ddagger} = 18.9 \pm 1.8$ kJ·mol^{-1}, $\Delta S^{\ddagger} = -138 \pm 5$ J·mol^{-1}·K^{-1}.

the $\Delta S^{\ddagger}$ value for k_1 in the sc-CO$_2$ system is more negative than that in o-C$_6$D$_4$Cl$_2$, as listed in Table 7. This is considered to be due to the formation of intermolecular interactions between unidentate hfacac and CO$_2$.[31,32]

The values of k_3 are larger than those of k_2 in both systems (Tables 6 and 7). This is reasonable, because the k_2 and k_3 pathways correspond to the coordination of Henol and DMSO to the vacant site in the intermediate II, and the DMSO molecule with smaller size and larger donicity than Henol (donor number (DN) of DMSO = 29.8, DN of Hacac = 20.0)[68] should more easily coordinate to such a site. The exchange reactions of DMSO in UO$_2$(hfacac)$_2$DMSO in o-C$_6$D$_4$Cl$_2$ and sc-CO$_2$ systems depend on [DMSO] and hence should proceed associatively as mentioned above. From this viewpoint, it is reasonable to presume that the values of k_3 are equal to or larger than the k_y and k_z values listed in Table 5 because the free DMSO should enter more easily the vacant site of the intermediate II in Scheme 1 compared with the association to complex I. On the basis of this assumption, the values of k_{-1} and k_2, which should be equivalent to or smaller than the real values, were estimated from the values of k_2/k_{-1} and k_3/k_2 in Tables 6 and 7 using the k_y and k_z values in Table 5. The results are listed in Tables 8 and 9 with the k_3 values. It is found that the k_2 and k_3 values in the o-C$_6$D$_4$Cl$_2$ system are about 250 and 25 times larger than those in sc-CO$_2$, respectively (Tables 8 and 9). These differences are also explained by the LA–LB interactions and the hydrogen bondings between free Henol or DMSO and CO$_2$ because such interactions should inhibit the associative entering of Henol and DMSO to the coordination site of intermediate II.

(68) Linert, W.; Fukuda, Y.; Camard, A. *Coord. Chem. Rev.* **2001**, *218*, 113−152.

Table 8. Values of k_{-1}, k_2, and k_3 in the o-C$_6$D$_4$Cl$_2$ System at Various Temperatures[a]

Temperature	k_{-1}	k_2	k_3[a]
°C	10^5 s^{-1}	10^6 M^{-1}·s^{-1}	10^7 M^{-1}·s^{-1}
40	0.915 ± 0.201	1.29 ± 0.07	1.18 ± 0.02
60	2.20 ± 0.40	2.24 ± 0.20	1.74 ± 0.02
70	2.97 ± 0.69	4.34 ± 0.94	1.91 ± 0.03
80	5.29 ± 2.49	6.23 ± 2.68	2.19 ± 0.03
90	11.2 ± 7.28	9.69 ± 5.60	2.50 ± 0.03
100	7.79 ± 4.72	7.42 ± 3.07	2.87 ± 0.02

[a] The assumption, $k_3 \geq k_y$.

Table 9. Values of k_{-1}, k_2, and k_3 in sc-CO$_2$ System at Various Temperatures[a]

Temperature	k_{-1}	k_2	k_3[a]
°C	10^4 s^{-1}	10^3 M^{-1}·s^{-1}	10^5 M^{-1}·s^{-1}
40	1.26 ± 0.49	4.97 ± 1.56	4.31 ± 0.23
60	1.92 ± 0.46	7.29 ± 1.60	7.08 ± 0.17
70	1.74 ± 0.48	7.34 ± 1.85	8.74 ± 0.12
80	2.84 ± 0.87	14.3 ± 4.15	10.7 ± 0.2
90	7.03 ± 1.65	28.4 ± 5.24	11.9 ± 0.2
100	8.65 ± 4.56	30.1 ± 15.2	13.3 ± 0.3

[a] The assumption, $k_3 \geq k_z$.

The values of k_{-1} and k_2 in the o-C$_6$D$_4$Cl$_2$ system are found to be larger than those in sc-CO$_2$ (Tables 8 and 9). This is also reasonably explained by the LA−LB interaction between CO$_2$ and Henol in the sc-CO$_2$ system, that is, the k_{-1} pathway should be blocked by the interaction of CO$_2$ between the end of the unidentate hfacac in the intermediate II, and the existence of the intermolecular interaction between Henol and CO$_2$ makes the approach of the relatively bulky Henol* to the intermediate II (k_2 pathway) difficult. Furthermore, the k_1 values in the o-C$_6$D$_4$Cl$_2$ system are much smaller than the k_2[Henol] values (8.04 × 10^3 to 6.51 × 10^5 s^{-1}), and those in the sc-CO$_2$ system are almost equivalent to k_2[Henol] values (4.51 × 10^1 to 2.26 × 10^3 s^{-1}). From these results, it is reasonable to consider that the rate-determining step in the exchange reaction of hfacac in UO$_2$(hfacac)$_2$DMSO in o-C$_6$D$_4$Cl$_2$ and sc-CO$_2$ is the ring-opening for one of two coordinated hfacac in UO$_2$(hfacac)$_2$DMSO.

Conclusions

In the present study, we have examined the structures of the UO$_2$(hfacac)$_2$DMSO complex in o-C$_6$D$_4$Cl$_2$ and sc-CO$_2$ and the ligand exchange reactions of UO$_2$(hfacac)$_2$DMSO in both media using ^{1}H and ^{19}F NMR spectroscopy. As a result, it was found that the UO$_2$(hfacac)$_2$DMSO complex in both media has a pentagonal bipyramidal structure, and that hfacac of UO$_2$(hfacac)$_2$DMSO coordinates to a uranyl moiety more strongly in o-C$_6$D$_4$Cl$_2$ than in sc-CO$_2$.

Furthermore, it was found that in both o-C$_6$D$_4$Cl$_2$ and sc-CO$_2$ systems the exchange rates of hfacac in UO$_2$(hfacac)$_2$-DMSO depend on [Henol] and decrease with an increase in [DMSO] and that the exchange rate constants of DMSO in UO$_2$(hfacac)$_2$DMSO depend on [DMSO]. From these results, it was proposed that the exchange reaction of hfacac in UO$_2$(hfacac)$_2$DMSO proceeds through the mechanism, where the ring-opening for one of two coordinated hfacac in UO$_2$(hfacac)$_2$DMSO is the rate-determining step, the resulting

vacant site is coordinated by the incoming Henol, followed by the proton transfer and the ring closure of unidentate hfacac. The rate constant at 60 °C and its activation parameters ($\Delta H^{\ddagger}$, $\Delta S^{\ddagger}$) for the ring-opening process are 35.8 ± 3.2 s^{-1}, 57.8 ± 2.7 kJ·mol^{-1}, and −42.9 ± 7.7 J mol^{-1}·K^{-1} for the o-C$_6$D$_4$Cl$_2$ system, and 518 ± 50 s^{-1}, 18.9 ± 1.8 kJ·mol^{-1}, and −138 ± 5 J mol^{-1}·K^{-1} for the sc-CO$_2$ system. The values of the rate constants corresponding to the ring closure of unidentate hfacac, the coordination of Hhfacac to the vacant site, and the DMSO exchange in the sc-CO$_2$ system are smaller than those in the o-C$_6$D$_4$Cl$_2$ one. It is proposed that such a difference is due to the existence of the solute−solvent interaction between Hhfacac or DMSO and CO$_2$ under supercritical conditions.